Bulletin of the Seismological Society of America, Vol. 94, No. 1, pp. 1–15, February 2004

On the Nature of an Unusual Wave Train Observed in the Northern Tien Shan Region

by Yu. F. Kopnichev and I. N. Sokolova*

Abstract We describe an unusual wave group that propagates in the Northern Tien Shan region along the border between mountain ranges and the Chu and Ili depressions to the north. This wave group, which we call S_L, stands out against the short-period coda on the recordings of local earthquakes and quarry explosions (at distances up to 100 km). The time t_m needed for the S_L group to reach maximum amplitude varies between 98 and 131 sec, and at the same time, the t_m value does not depend on epicentral distance. At distances up to 30 km, the S_L group has a very narrow spectrum (T = 1.5–1.8 sec), but when the epicentral distance increases, the predominant period also increases up to approximately 2.3 sec (at $\Delta \sim 100$ km). Characteristics of the wave group are significantly different for the Zaili fault zone than for the regions to the west of 76° E and to the east of 79° E. In the Zaili fault region, the S_L group is characterized by great variability of velocity, amplitude, and polarization parameters even for nearby paths. The S_L group maintains an amplitude within 0.7 of its maximum for 4–36 sec depending on the path. The polarization of the S_L group is in the vertical plane in the Zaili fault-zone region and in the horizontal plane in other regions. Particle motion is elliptical or almost circular. We suggest that the S_L group consists of shear waves propagating in a subvertical wave guide and reflected from a thin upper mantle layer.

Introduction

During the study of characteristics of short-period wave fields in the Northern Tien Shan region, an abnormal wave group was distinguished, which can be clearly seen on the background of the *S* coda on the recordings of local earthquakes and quarry explosions. We are not familiar with any publications where similar wave groups observed in other regions are described. The present study investigates the characteristics of this wave group, based on an analysis of a large amount of data, received from analog and digital seismic stations.

Geological and Geophysical Characteristics of the Region under Investigation

The region under investigation is part of the Northern Tien Shan. The Chu and Ili depressions, separated by low Kendyktas mountains, with a maximum height of 2400 m (Fig. 1), are situated in the north of the region. In the south, the Chu depression is bordered by the Kirgiz range and is separated from it by the Chonkurchak deep fault zone. The southern part of the Ili depression joins the rising Zaili Alatau range and is separated from it by the Almaty and Zaili deep fault zones. The eastern part of the region is constrained on the south by the Ketmen' range, which is up to 3500 m high, and is separated from it by North Ketmen deep fault zone. The Zaili Alatau range stretches in the east-northeast direction, and the highest points here reach about 5000 m. In the south, this range ends up with the Chilik-Kemin graben, which separates it from the Kungei Alatau range. The Issyk Kul depression is situated in the south, which is stretched in a sublatitude direction.

The maximum thickness of young sedimentary rocks in the Ili depression region reaches 4200 m (in the central part of the Almaty depression, near station AA3 [Fig. 2]) (Gal'perina *et al.*, 1985). Thus the total vertical component of neotectonic motion on the border of the Northern Tien Shan and Ili depression is about 9 km. The thickness of sedimentary rocks in the northern part of the Chu depression, which abuts against the Kendyktas range, and in the southern edge of the Ili depression, which borders the Ketmen' range, is much lower: 200 and 500 m, respectively (Krestnikov *et al.*, 1979).

The depth of the Moho increases from north to south from 45–50 km in the Kendyktas region and southern outskirts of the Ili depression to 55–60 km in the regions of

*Present address: KNDC IGR NNC, Chaikina Str. 4, Almaty, Kazakhstan 480020; sokolova@kndc.kz (I.N.S.).

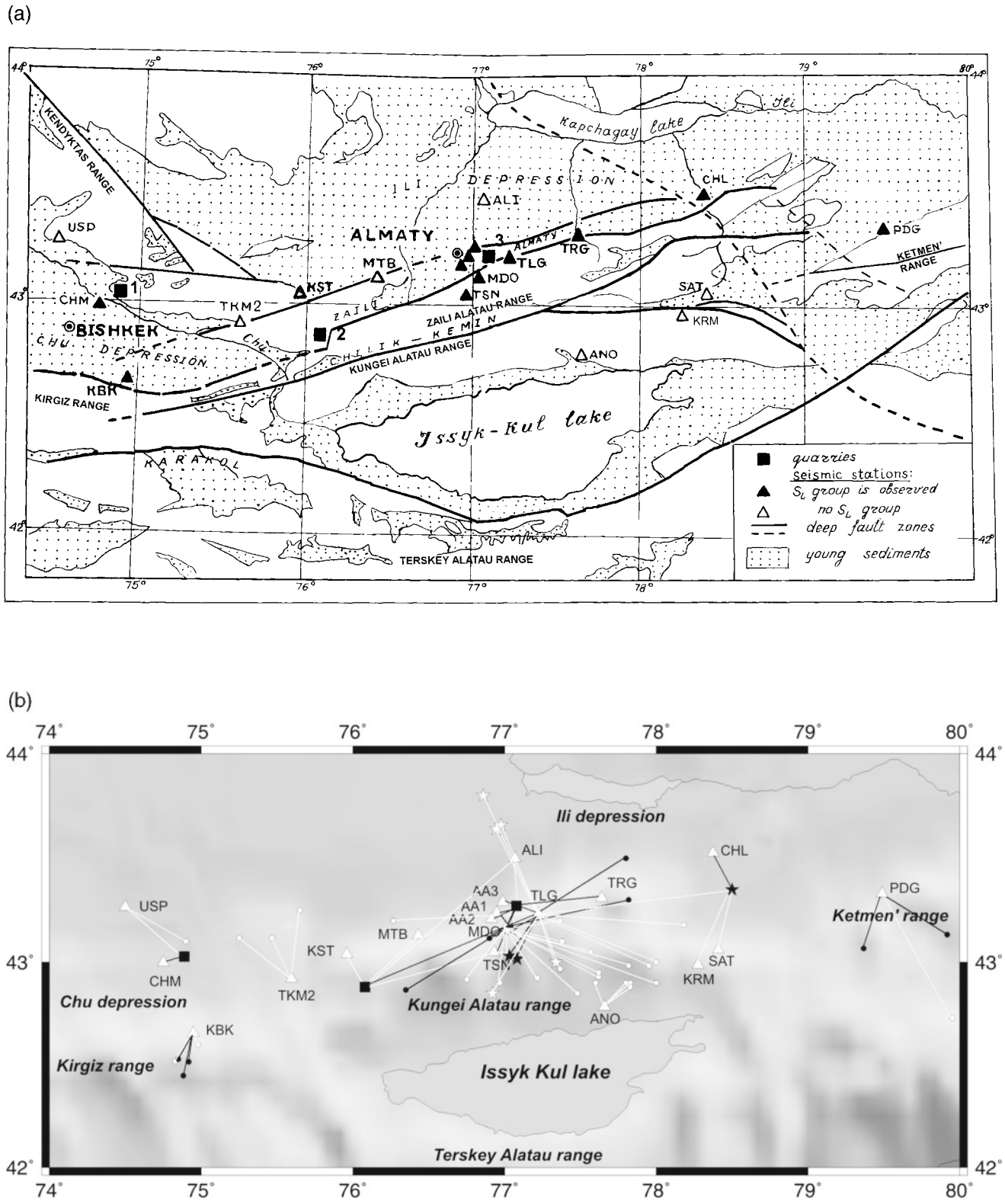

Figure 1. (a) A map of the region under investigation. Quarries: 1, Aglatas; 2, Aktyuz; 3, Kotur-Bulak. (b) A map of paths for which S_L is observed (black lines) and is not observed (white ones). Squares are quarries. Circles and stars denote epicenters of earthquakes and explosions, respectively (black symbols, S_L is identified for some paths; white ones, no S_L). Triangles are seismic stations. Note: S_L was not found for many stations to the north of ALI and to the south of the KBK–ANO line, which are not shown in the figure.

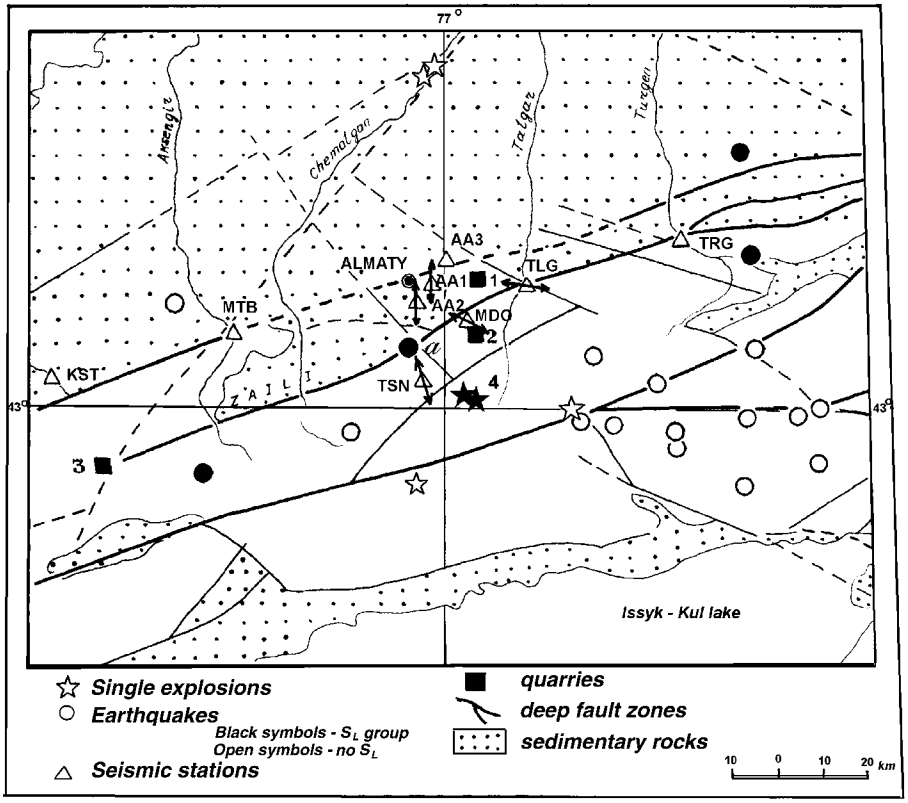

Figure 2. Observation system in Zaili fault region. Quarries: 1, Kotur-Bulak; 2, Medeo; 3, Aktyuz; 4, Big Almaty Lake; a, epicenter of earthquake of 4 March 1991. The arrows on the triangles show directions of S_L group arrivals to the corresponding station for Kotur-Bulak quarry explosions.

Kirgiz, Zaili, and Kungei Alatau and also the Ketmen' ranges (Gal'perina *et al.*, 1985).

The Chu and Ili depressions are characterized by rather low heat flow, which does not exceed 45 mW/m^2. The Kendyktas, Zaili, and Kungei Alatau regions are characterized with higher values of heat flow (more than 100 mW/m^2). The maximum values of heat flow correspond to the active fault zones and in particular to the Zaili fault (Vilyaev, 1994).

Data

We analyzed data received by permanent and temporary stations of the Complex Seismological Expedition of the Joint Institute of Physics of the Earth, Russian Academy of Sciences, Institute of Seismology, National Academy of Sciences of Republic of Kazakhstan, and the International Research Center geodynamic proving ground in Bishkek (Fig. 1). The stations are equipped with short-period three-component analog SKM-3 stations and Refraction Technology, Inc. (REFTEK) digital stations with the corresponding bandwidth between 0.7–10 and 0.03–20 Hz. The stations are installed in the mountains on bedrock and on sedimentary rocks, up to 4200 m thick, in the Ili depression region (CHL, ALI, AA1, AA2, and AA3). (Stations AA3 and ALI are located in boreholes at depths of 1000 and 800 m, respectively [Gal'perina *et al.*, 1985]). The elevation of stations above sea level varies from 550 m (ALI) to 3000 m (TSN).

The recordings of local earthquakes and quarry explosions at epicentral distances up to 100 km were processed. Special emphasis was made on the use of recordings of explosions, where the accuracy of hypocentral coordinates is much higher than for the local earthquakes. The largest amount of data corresponds to the seismograms of explosions at the small Kotur-Bulak quarry, situated in the mountains to the east of Almaty, Aktyuz quarry (80 km to the southwest of Almaty), and the Aglatas quarry, which is situated on the southwestern edge of the Kendyktas range (Fig. 1). Several hundred seismograms were processed.

Analysis of Experimental Data

Data Processing Technique

Considering the characteristics of experimental data, in many cases narrowband frequency filtering of data was used. The filters were used with central frequencies at 0.45, 0.6, and 1.25 Hz and a bandwidth of 2/3 of an octave at 0.7 of maximum level (similar to corresponding frequency selecting [CHISS in Russian] filters [Rautian and Khalturin, 1978]).

First, let us examine the data from the Zaili fault zone, for which the largest amount of data was acquired.

Zaili Fault Zone

The research showed that, for many cases, on the recordings of local events for the paths close to this fault (mainly at epicentral distances up to 30 km), an unusual wave group could be clearly observed on the background of the *S* coda. Let us name it S_L. The elapsed time t_m when the amplitude of the group reaches maximum varies from 105 to 131 sec. The minimum t_m values (105.0 sec) correspond to the explosion recordings for the Kotur-Bulak–AA3 path, and the maximum value (130.6 sec) corresponds to the earthquake seismogram of 4 March 1991 with the source situated on the Zaili fault axis (to the north of station TSN), recorded by station MDO (Tables 1 and 2; Fig. 2).

It is important to note that very large deviations of the form of this group can be observed even for short paths. For the explosions at the Kotur-Bulak quarry, recorded by stations AA1, AA2, AA3, MDO, and TSN, the S_L group, as a rule, is a compact train of oscillations with a duration of 3–4 cycles (5–6 sec), which clearly stands out against the short-period coda background (Figs. 3 and 4). For other paths (Kotur-Bulak–TLG and especially Medeo [quarry]–TLG and Medeo–AA1), this group smears a lot and its level with respect to the coda sharply decreases (Figs. 5 and 6). Figure 7 shows the dependence of relative duration τ of this group (an envelope in which amplitudes remain above 0.7 of their maximum level) versus the S_L- to *S*-wave amplitude ratio (A_{SL}/A_S) at small distances (<30 km). One can see a clear negative correlation between these values: the increase of τ leads to the decrease of A_{SL}/A_S and vice versa. In this case, both values change by 1 order of magnitude (from 3.8 to 36 sec and from 0.014 to 0.14, respectively).

On the recordings of Kotur-Bulak quarry explosions, received by the station at MDO, one can see that at small distances the visible periods in the group on average decrease by 1.8–1.5 sec from the first cycle to the last (Fig. 3). The periods T_m, corresponding to the maximum amplitudes at distances up to 30 km, are practically identical for different paths (T_m = 1.6–1.7 sec; see Figs. 3–6, Table 1).

The apparent velocities of the S_L group are very small, less than 100 m/sec for Kotur-Bulak–AA1, Kotur-Bulak–AA3, and Aglatas–CHM paths. At the same time, visible interval velocities c_{int} are much greater; they vary from 1.0 km/sec (AA3–MDO path) to 2.6 km/sec (TLG–MDO) (see Table 3). It is important to note that for the AA3–MDO and AA3–TSN paths, which mainly go through the mountains, the c_{int} values are considerably lower than group velocities of Rayleigh waves with a period of T = 1.6 sec (which according to our data for the Northern Tien Shan region are equal to 2.0–2.2 km/sec). At the same time for AA3–AA1 and AA1–AA2 paths, which go through sedimentary rocks only with an *S*-wave average velocity of about 1.3 km/sec in the upper 2-km layer (Gal'perina *et al.*, 1985), the interval velocities are even higher than for the AA3–MDO path. Note, c_{int} values for the TLG–MDO and MDO–TSN paths are a little bit higher than *S*-wave velocities in the uppermost layers of the Earth's crust in the Zaili Alatau range region (c_s = 2.4 km/sec, according to V. I. Shatsilov's data, personal comm.).

Based on the available data, we can trace the S_L group to distances at least up to 100 km. Figure 8 shows an example of a seismogram of an Aktyuz quarry explosion, the path from which to station TLG (Δ = 100 km) mainly goes through the Zaili fault zone (Table 1, Fig. 1). In this case, the S_L group is a smeared-out train of oscillations with a duration of 7–8 cycles and the visible periods increase up to 2.3 sec.

With increasing distance, the A_{SL}/A_S ratio grows sharply

Table 1

t_m and T_m Values for Different Paths (According to Recordings of Explosions)

Path	Δ (km)	t_m (sec)*	T_m (sec)
Kotur-Bulak–AA1	11	110.3 ± 0.8 (28)	1.60 ± 0.10
Kotur-Bulak–AA2	13	113.6 ± 0.3 (9)	1.56 ± 0.10
Kotur-Bulak–AA3	8	105.0 ± 0.6 (7)	1.61 ± 0.06
Kotur-Bulak–TLG	12	113.0 ± 0.4 (58)	1.70 ± 0.07
Kotur-Bulak–MDO	12	119.4 ± 0.5 (78)	1.68 ± 0.04
Kotur-Bulak–TSN	27	125.8 ± 0.4 (31)	1.68 ± 0.07
Kotur-Bulak–TRG	45	124.0 ± 0.5 (8)	1.79 ± 0.06
Medeo–TLG	15–19	128.6 ± 0.5 (4)	1.60 ± 0.10
Medeo–AA1	15	130,1	1,6
Lake–TLG†	26–27	125.6 ± 0.3 (2)	1.70 ± 0.05
Lake–MDO†	15–16	–	–
Lake–TSN†	8–9	–	–
Aktyuz–KST	22	–	–
Aktyuz–MTB	40	–	–
Aktyuz–TLG	100	118.3 ± 1.6 (35)	2.30 ± 0.16
Aglatas–CHM	10	102.7 ± 0.5 (6)	1.47 ± 0.04

*Standard deviations and number of events (in parentheses) are shown.
†Explosions in the Big Almaty Lake region.

Table 2
Earthquakes for which the S_L Group was Identified

Date (mm.dd.yy)	t_0 (hh-mm-ss)	φ	λ	h (km)	K*	Station
04.08.86	08-22-05.0	42° 52′	76° 21′	11	10.5	MDO
06.01.87	07-23-37.1	43° 18′	77° 49′	20	10.9	MDO
03.04.91	03-56-51.0	43° 07′	76° 54′	5	9.4	MDO
02.28.92	19-47-29.8	43° 30′	77° 48′	15–20	9.9	TLG
09.07.94	18-08-58.4	42° 31′	74° 55′	10	9.3	KBK
01.14.96	18-16-26.8	42° 45′	74° 53′	–	11.8	KBK
12.25.97	14-16-56.8	43° 04′	79° 22′	–	7.7	PDG
02.09.98	13-46-36.0	42° 32′	74° 51′	5	9.4	KBK
02.24.98	04-20-47.6	43° 08′	79° 55′	–	7.8	PDG

*Energy class.

(Fig. 8), so that for the Aktyuz–TLG path it becomes greater than 1 (at $T \sim 2.3$ sec). Note that the amplitude ratio of the S_L group to regular Rayleigh waves for this path is also close to 1.

We should note that this group stands out only for the paths that are situated close to the Zaili fault zone. From Figures 1–6 and 8 and Table 1, this can be seen most clearly when the middle of the path is situated no more than 5 km from the fault's axis ($\Delta < 30$ km). When its distance from the axis is more than 8–10 km, the S_L group does not show up on the recordings for the epicenters located both to the north of the fault, in the Ili depression region, and to the south, in the Zaili Alatau region (Figs. 1, 2 and 9).

The acquired data prove a sharp change of velocity and amplitude characteristics of short-period wave fields while crossing the Zaili fault. From Figure 9 and Table 1, we can see that t_m values for the paths to the north of the fault are on average less by 15–20 sec than those for the paths located to the south of the fault. A consistent increase of t_m values while approaching the fault axis can be observed, which is several times more rapid for the northern paths. For the paths crossing the fault zone, t_m values have intermediate values and large scatter.

An analysis of polarization characteristics of the S_L group was conducted. From Figures 10 and 11, one can see for the paths going near the Zaili fault region an elliptical polarization in the vertical plane of the S_L group, similar to that of Rayleigh waves. At the same time, the arrival direction of these waves is extremely unstable and changes sharply even between the nearby stations. The predominant polarization plane of the S_L group is usually different from the ray plane. So, taking into consideration the velocity characteristics of the S_L group, we can conclude that for the paths from Kotur-Bulak quarry, these waves approach stations AA1 and AA2 from the north and stations TLG and MDO from the west or northwest (assuming that this group arrives at the stations as Rayleigh waves).

Regions to the West of 76° E and to the East of 79° E

The northern and southern edges of the Chu depression are other regions where the S_L group stands out very clearly. But here characteristics of this wave differ significantly from the Zaili fault region. In Figure 12, one can see that the S_L group from the explosions on Aglatas quarry, detected by station CHM, is horizontally polarized and the major axis of the polarization ellipse almost coincides with the azimuth to the epicenter. The S_L group on the recordings of nearby earthquakes received by station KBK is polarized in a similar way.

To the east of 79° E, we could find the S_L group only on the PDG station recordings. As one can see in Figure 13, in this case, similar to the region to the west of 76° E, the S_L group is polarized horizontally and the angle of major axis of the ellipse is close to the azimuth to the epicenter. We should note that for the paths to the west of 76° E and to the east of 79° E, one cannot observe even very weak dispersion of the S_L group as for the Zaili fault region (see Figs. 3 and 14).

Figure 15 shows a dependence $t_m(\Delta)$ for the whole region under investigation. One can see that with this large dispersion of data, no dependence of t_m values on distance can be established. At the same time, the figure shows that the values of this parameter for the paths located to the west of 76° E are significantly lower (usually by 15–20 sec) than to the east of this meridian.

Figure 16 shows a dependence of T_m values versus distance. We can see a consistent increase of visible periods in the S_L group with distance, and again T_m values for the western paths are lower than the eastern ones (by about 10%).

Discussion

On the Origin of S_L Group

First we should note that the S_L group stands out only at the stations located on the borders between the Northern Tien Shan mountain structures and adjoining depressions (Chu and Ili). We could not find this group (at least not yet) at the stations located relatively far from these borders (ALI, ANO, KRM, SAT, and many others located to the north of station ALI and to the south of the KBK–ANO line, which are not shown in Figs. 1–2).

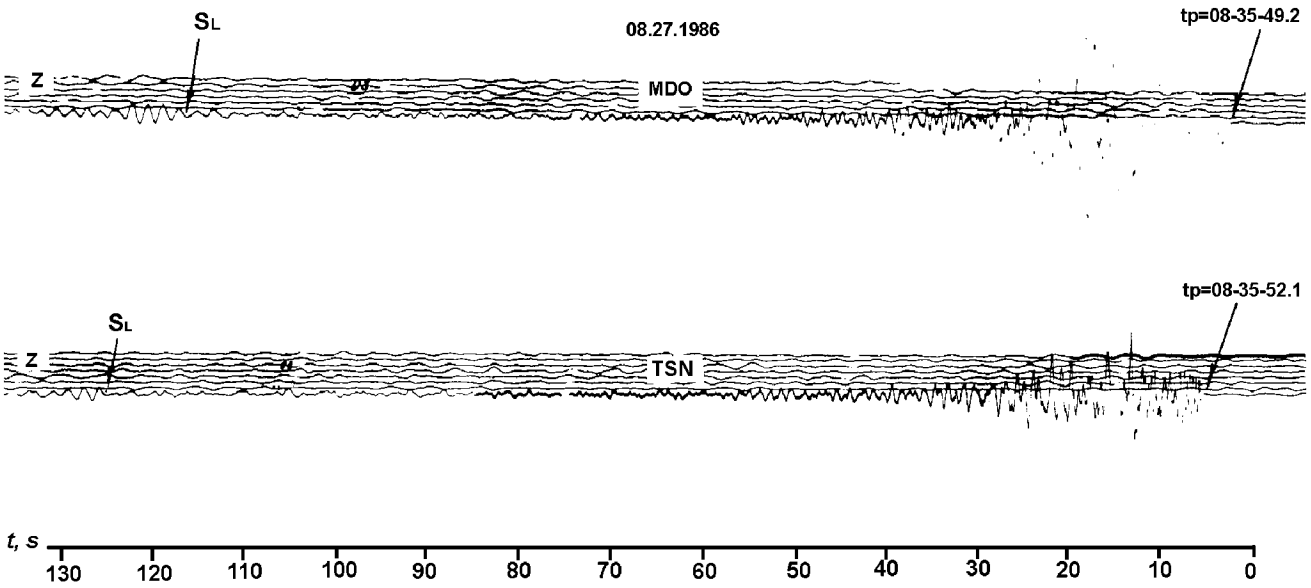

Figure 3. Seismograms of Kotur-Bulak quarry explosion. Stations MDO and TSN, SKM-3. t_p is the time of *P* arrival (in Figs. 3–6).

First, let us discuss the possible mechanisms by which the S_L group is formed in the Zaili fault region. Formation of this group by surface waves is one possible mechanism. Very low apparent velocities support the fact that the S_L group definitely cannot be formed by direct Love or Rayleigh waves.

A hypothesis of formation of this wave group by surface waves reflected from some remote border in the upper part of the Earth's crust contradicts, in particular, the observed polarizations. In this case, the S_L group should have approximately the same polarization at the different stations from the Kotur-Bulak quarry explosions. Besides that, as we have seen before, the S_L group interval velocities for some paths are much lower than Rayleigh-wave group velocities. Furthermore, due to strong attenuation and scattering in the upper part of the Earth's crust, the reflected waves cannot have amplitudes close to those of regular Rayleigh waves (for the Aktyuz–TLG path, see Fig. 8). Finally, t_m values of the reflected surface waves definitely could not increase when the paths approach the Zaili fault axis from the north and from the south.

Formation of the group by multiple reflections of *S* waves from the Moho boundary is impossible due to weak intensity of secondary waves. Finally, the scheme of S_L group formation by reflected longitudinal waves contradicts its polarization characteristics.

The following circumstance is of great importance for interpretation of experimental data. Earlier a detailed analysis of short-period *S* coda using recordings of local quarry blasts and earthquakes in the area of transition from the Zaili Alatau range to the Almaty depression was carried out (Kopnichev, 2000). It was shown that the coda *Q*-value (for the frequency of 1 Hz), determined by coda envelope decay, over the interval of $t = 20$–70 sec changes from 55 to 560 at a distance of ~10 km between paths. (Note that this effect confirms once more the conclusion on the coda formation for the frequencies of ~1 Hz by shear waves reflected from multiple subhorizontal boundaries in the Earth's crust and upper mantle in the Central Asia region [Kopnichev, 1985; Aptikaeva and Kopnichev, 1993].) On the basis of this analysis, a narrow strip of very high *S*-wave attenuation, extending to a depth of ~150 km beneath the Zaili fault, was identified. Attenuation sharply decreases to the north of the fault zone, beneath the area of maximum thickness of sedimentary rocks in the Almaty depression, and becomes considerably weaker to the south of the fault, beneath the Zaili Alatau range. Essentially, the sharp temporal variations of coda envelopes at $t < 135$ s are connected with this zone of high attenuation. The structure of the attenuation field varies to depths up to 200–250 km, due to active migration of fluids (Kopnichev and Sokolova, 1997; Kopnichev, 1998). Based on these data, Kopnichev (2000) concluded that the Zaili fault is a subvertical wave guide for short-period shear waves.

Note that a similar structure of the lithosphere is observed in the region of the Altyn Tagh fault, at the southern border of the Tarim massif. Tomographic inversion of *P*-wave teleseismic travel-time residuals reveals a steep and narrow low-velocity zone extending to 140 km beneath this fault (Herquel *et al.*, 1999).

Starting from here, we suppose that finding the S_L group is connected with propagation of shear waves in the subvertical wave guide. In order for this group to return back to the surface, it should be reflected from an impedance contrast due to heterogeneity in the upper mantle. The stability of periods and very narrow spectrum of the S_L group at short

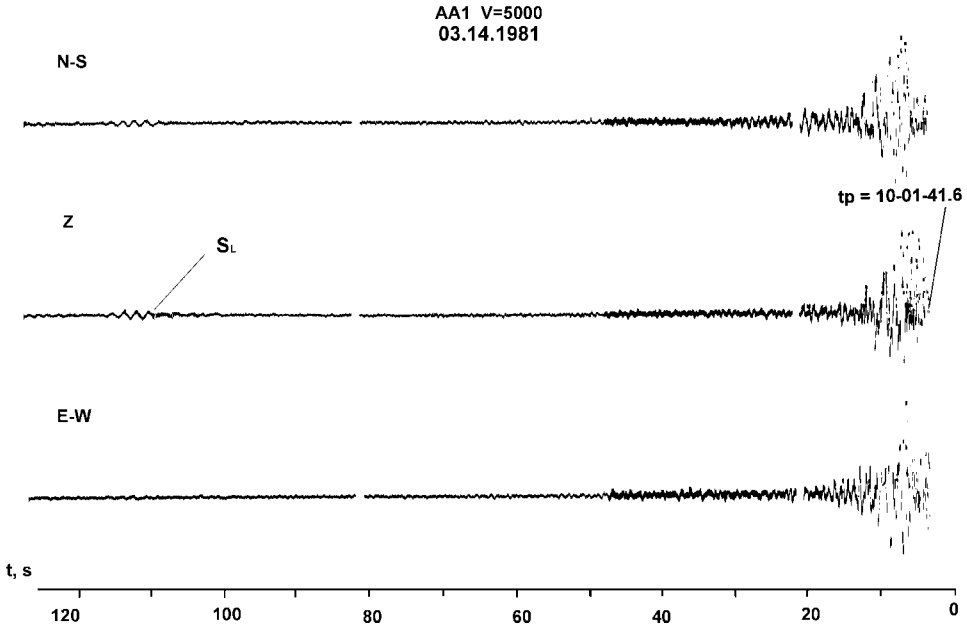

Figure 4. Seismogram of Kotur-Bulak quarry explosion. Station AA1, SKM-3. *V* is a magnification (in Figs. 4 and 6).

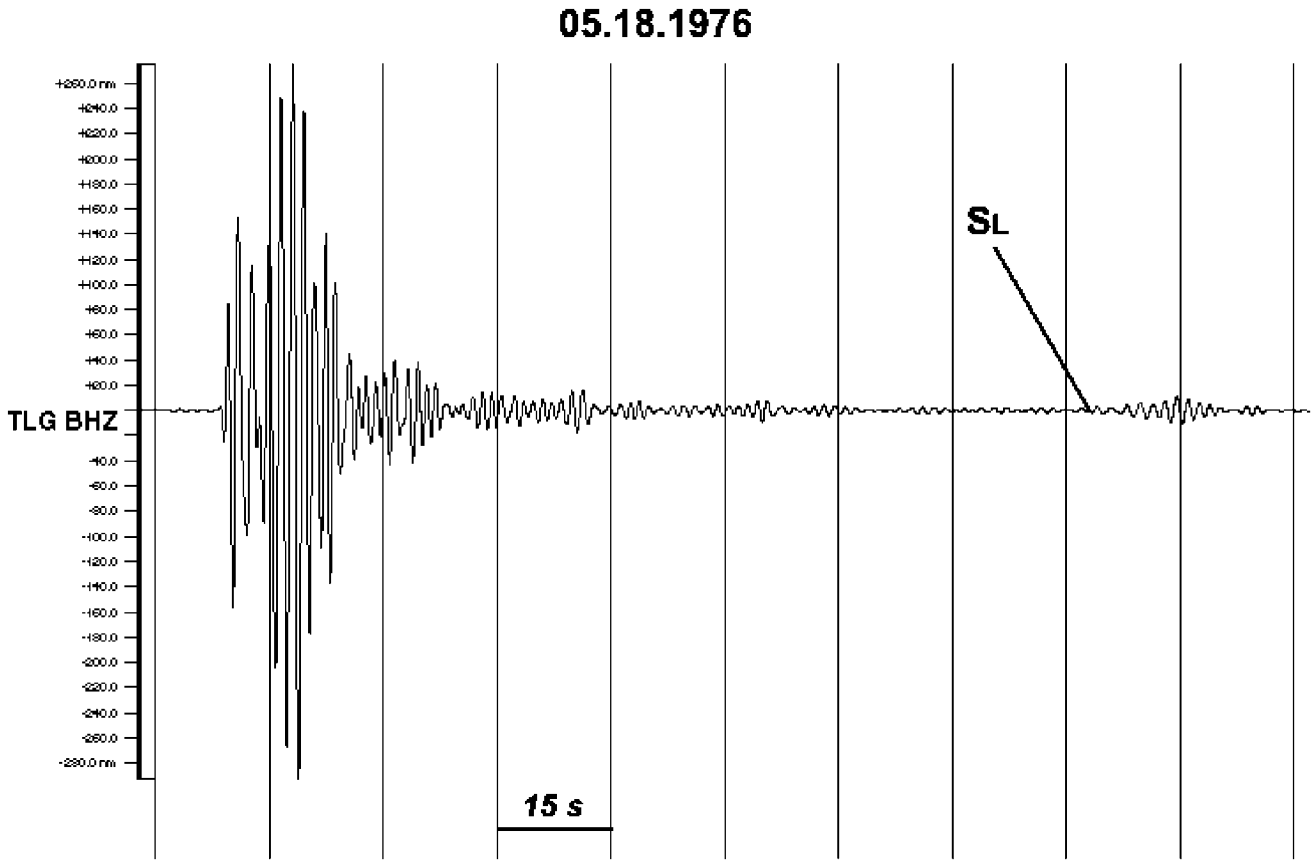

Figure 5. Seismogram of an explosion in Medeo region (18 May 1975). Station TLG, 0.6-Hz filter.

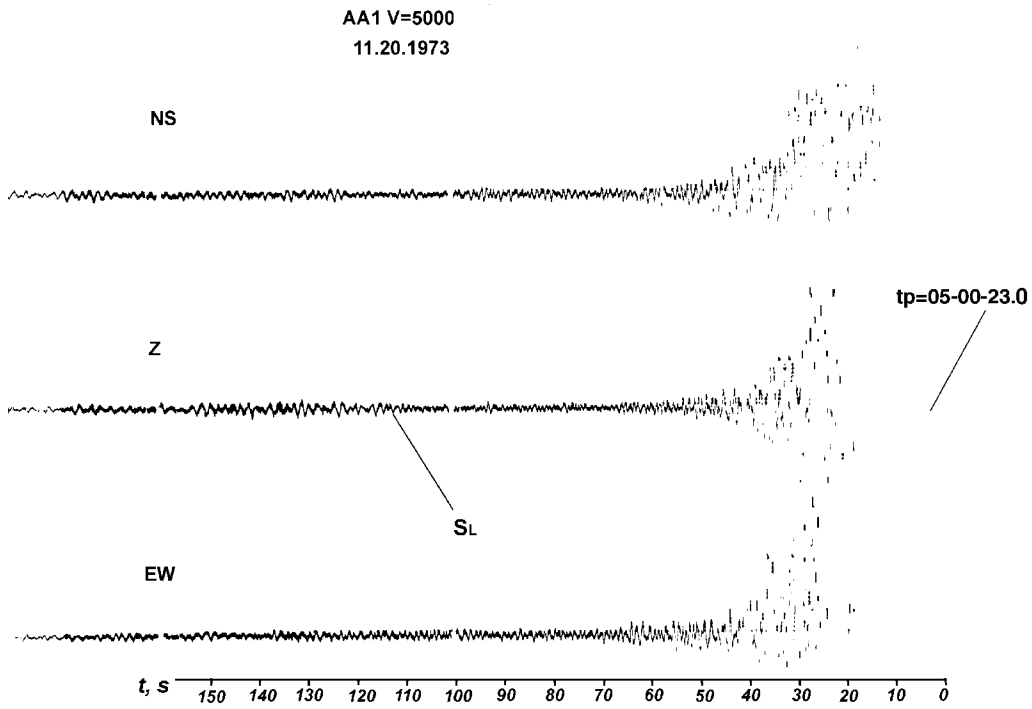

Figure 6. Seismogram of an explosion in Medeo region. Station AA1, SKM-3.

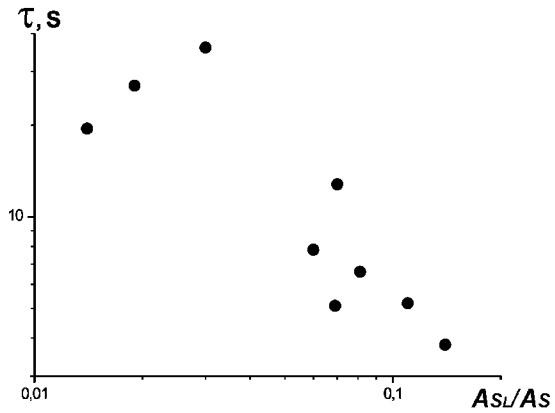

Figure 7. Relative duration of S_L group at 0.7 of maximum level versus S_L- to S-wave amplitude ratio (according to data for different paths).

distances, and the gradual increase of period with increasing distance (considering that t_m values and, consequently, the path, passed by S-waves, practically do not change), support the fact that most likely shear waves are reflected from a rather thin layer.

So, we formulate the following hypothesis: the S_L group represents shear waves propagating in a subvertical wave guide connected to the Zaili fault zone and reflected from a thin upper mantle layer, which we call the L layer. Let us examine how experimental data fit this hypothesis.

First, we list the characteristics of signal propagation through a wave guide (Brekhovskih, 1974). We assume that the velocity of S waves increases from the axis to the edges of the wave guide.

1. Refraction of rays crossing the wave guide axis (Fig. 17). The paths of the rays and the amount of trapped energy depend on the location of the source with respect to the wave-guide axis. In general, the waves from sources located outside of the wave guide are not trapped.
2. Much weaker geometric spreading in the wave guide in comparison with homogeneous half-space (without attenuation).
3. Existence of convergence zones with sharp increase of signal amplitude and shadow zones, where we can find only scattered energy.

First note that kinematic characteristics of the S_L group could be a strong argument for the suggested hypothesis, because the largest travel times t_m correspond to the paths that lie near the fault axis; t_m values decrease with increasing distance from the fault axis, especially in the north direction. (Such a distribution of t_m values is typical for the vertical wave guide with the lowest velocities in the central part of it [Brekhovskikh, 1974].)

The existence of a subvertical wave guide also explains why the S_L group usually cannot be observed for sources more than 10^{-15} km away from the Zaili fault. In this case, the shear waves just cannot be trapped by the wave guide.

Sharp differences in relative S_L levels and t_m times even for nearby paths correspond to the existence of convergence and shadow zones in the wave guide (Brekhovskih, 1974).

Table 3
Interval Velocities of S_L Group for Some Paths (Explosions at Kotur-Bulak Quarry)

Path	AA3–AA1	AA1–AA2	AA3–MDO	AA3–TSN	TLG–MDO	MDO–TSN
c_{int} (km/sec)	1.3	1.4	1.0	1.3	2.6	2.5

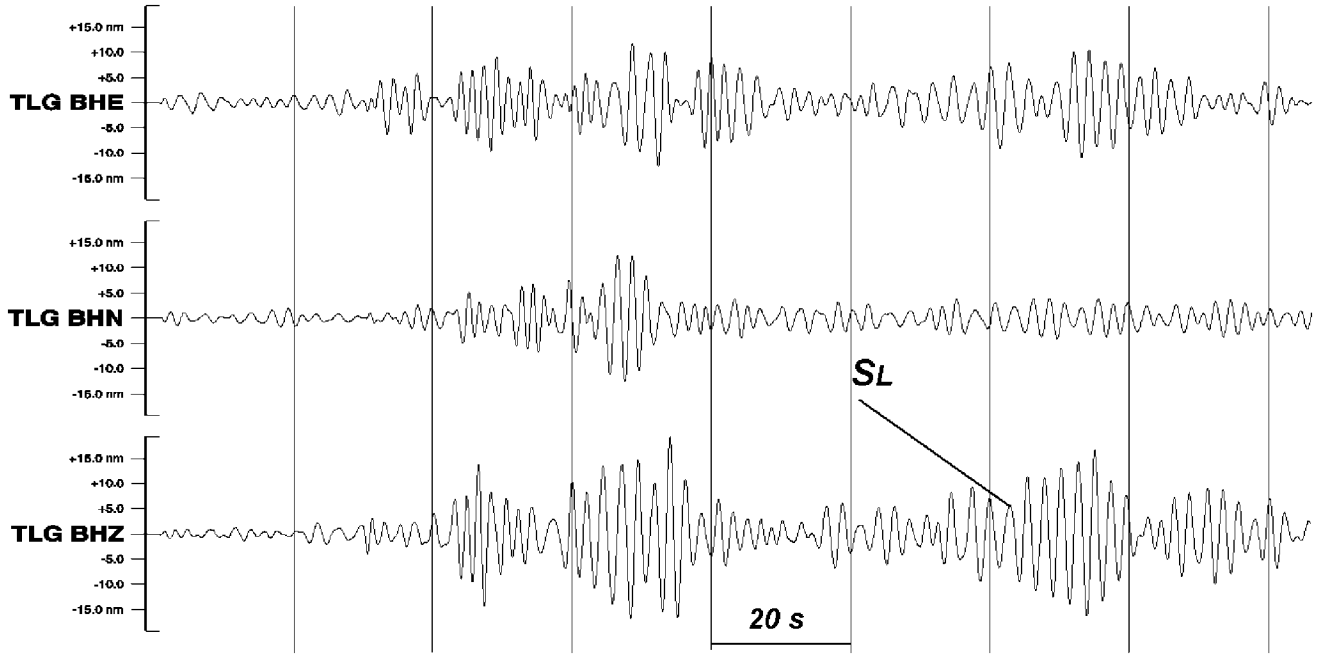

Figure 8. Seismogram of Aktyuz quarry explosion. Station TLG, 0.45-Hz filter.

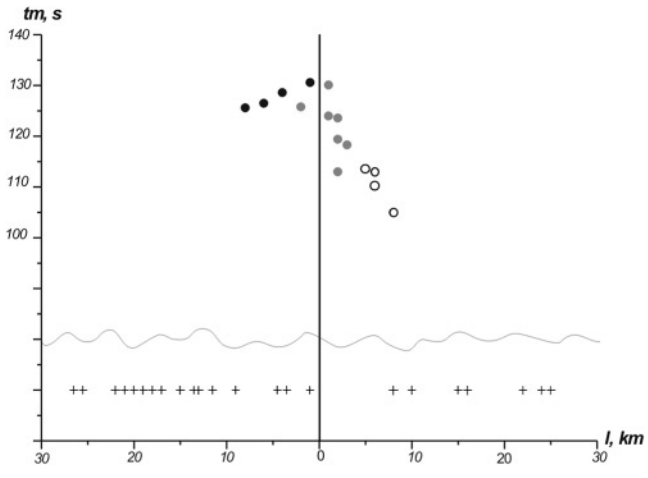

Figure 9. t_m values versus the distances between middles of the paths and the Zaili fault axis. Black circles show paths to the south of the Zaili fault, open ones to the north of the fault. Gray circles indicate the paths intersecting the fault. Crosses are paths for which no S_L was identified.

This is also proved by inverse correlation between τ and A_{SL}/A_S values: in the shadow zones, where mostly scattered waves arrive, the amplitude of the signal should decrease and its relative duration should increase.

One should note that judging by the obtained data, the width of the subvertical wave guide does not exceed 20–25 km. This is indicated by the distribution of sources and stations in space where the S_L group can be observed (Figs. 1, 2). Besides, the analysis of t_m values shows that the northern boundary of the wave guide is much sharper than the southern one.

Peculiarities of the region of transition between the Zaili Alatau range and the Almaty depression are large relief contrast and a low-velocity sedimentary layer with irregular interface. As shown by Hill and Levander (1984) and Levander and Hill (1987), an effective conversion of deep S waves to surface waves occurs in such conditions. This allows us to explain some other characteristics of the S_L group. For example, low apparent velocities, small dispersion, and polarization of the S_L group in the Zaili fault area imply that it propagates near the surface as Rayleigh waves. At the same time, taking into account strong attenuation and scattering of short-period surface waves due to heterogeneity in

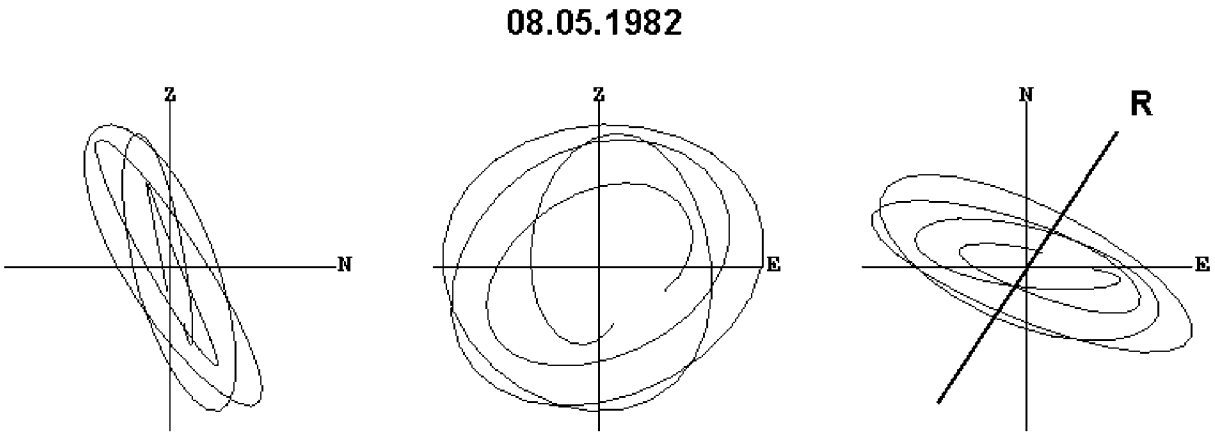

Figure 10. Polarization of S_L group. (R denotes the direction to the epicenter [in Figs. 10–13]). Kotur-Bulak quarry explosion. Station MDO, SKM-3.

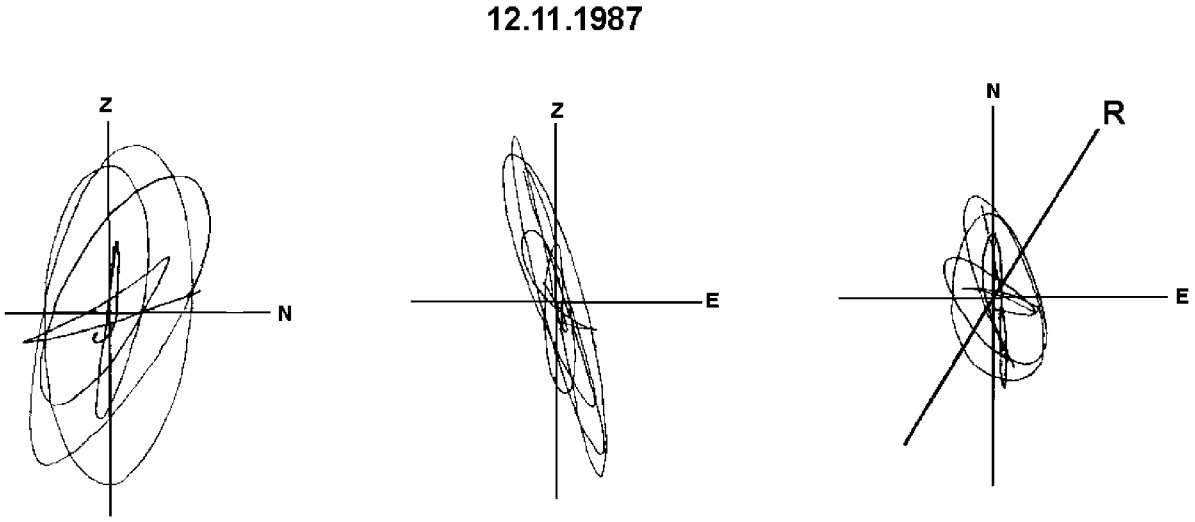

Figure 11. Polarization of S_L group, Kotur-Bulak quarry explosion. Station TSN, SKM-3.

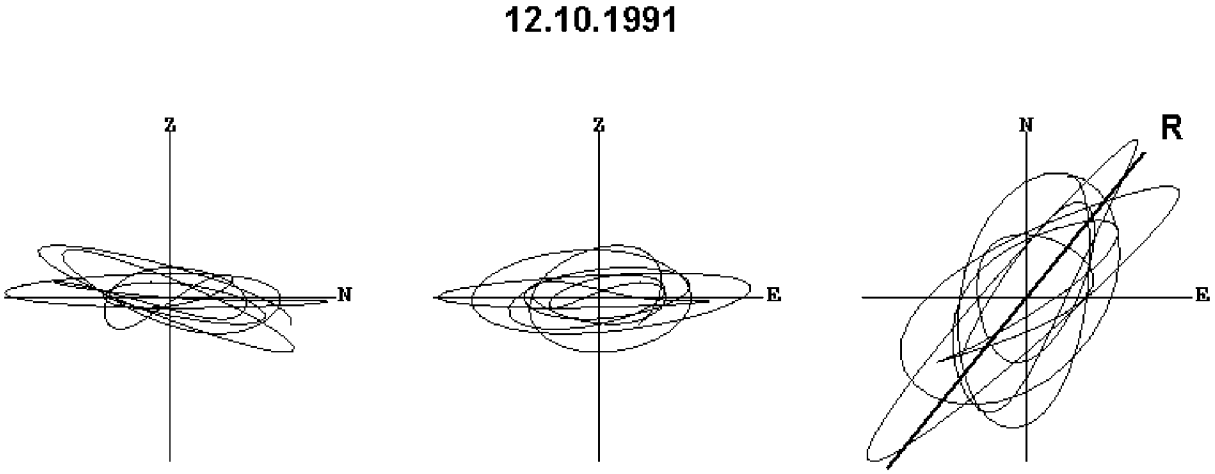

Figure 12. Polarization of S_L group, Aglatas quarry explosion. Station CHM, REFTEK.

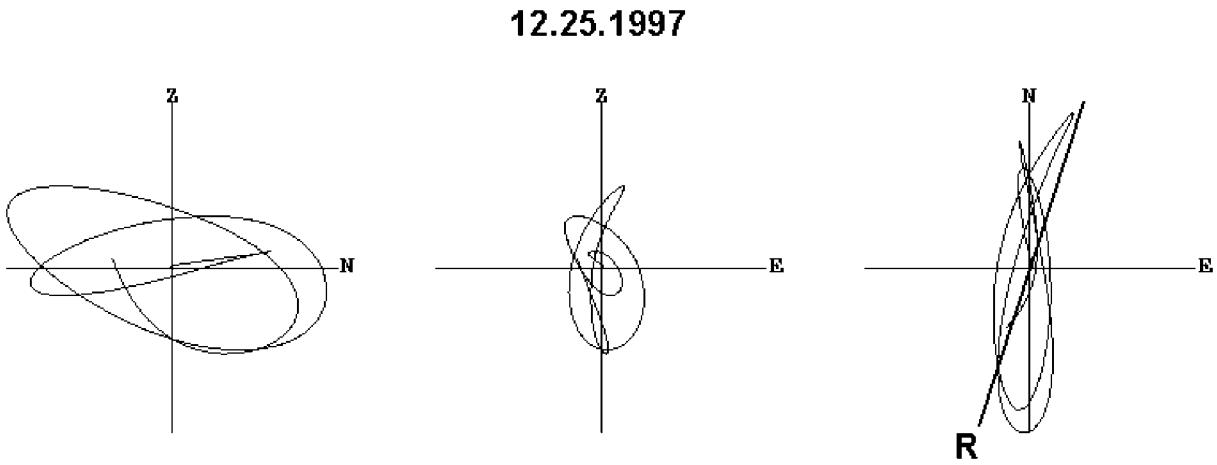

Figure 13. Polarization of S_L group, the earthquake of 25 December 1997 (Table 2). Station PDG, REFTEK.

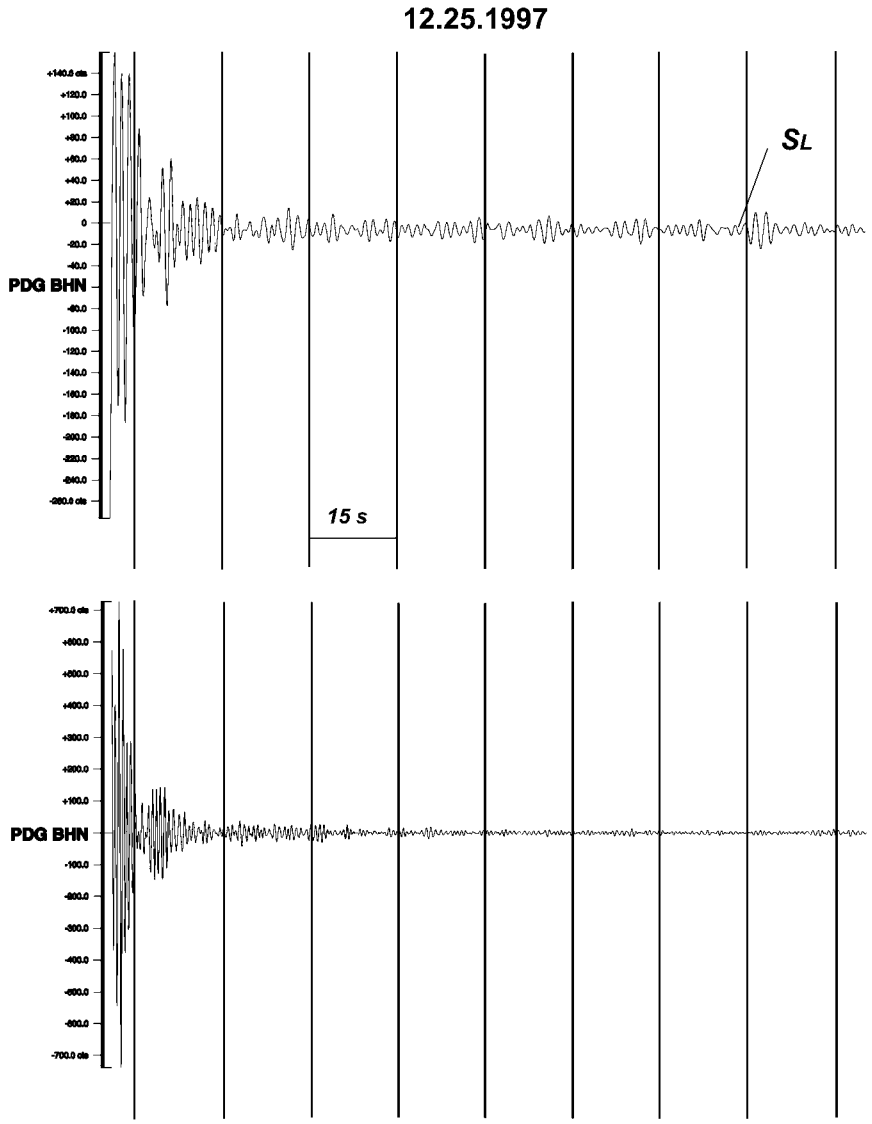

Figure 14. Seismogram of the local earthquake (25 December 1997). Station PDG, 0.6- and 1.25-Hz filters.

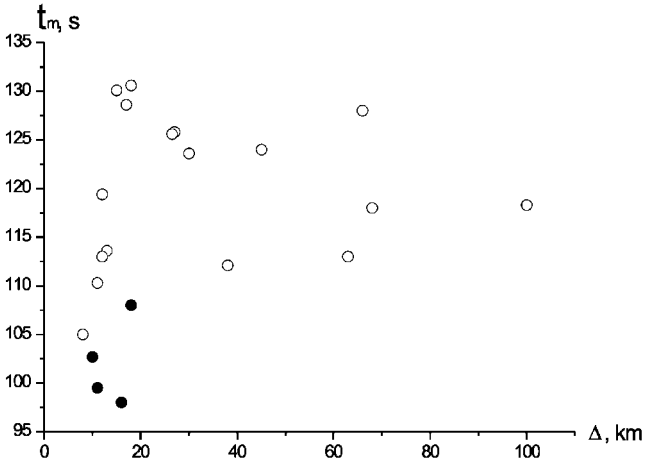

Figure 15. $t_m(\Delta)$ dependence for S_L group. Open symbols represent paths to the east of 76° E, black symbols to the west of 76° E (in Figs. 15, 16).

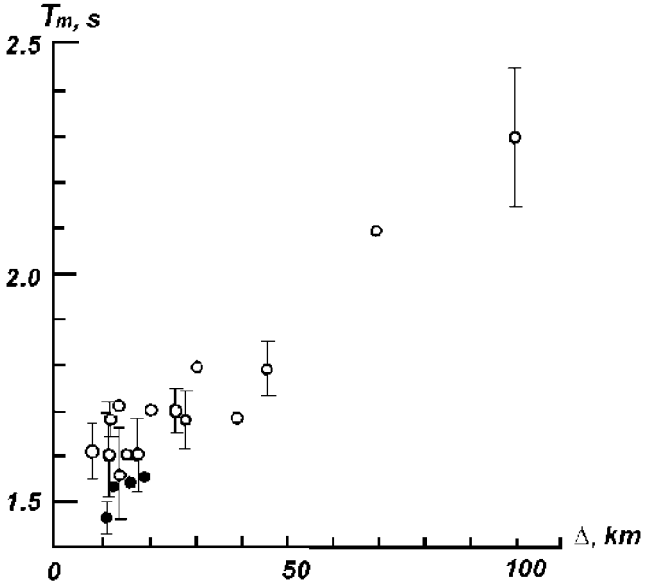

Figure 16. $T_m(\Delta)$ dependence for S_L group. Error bars are standard deviations.

the Zaili zone, one can believe that the conversion of *S* to *R* waves occurs at a relatively small distances from recording stations.

Accepting the suggested hypothesis, we can naturally explain the peculiarities of the S_L group to the west and to the east of the Zaili fault zone. Taking into consideration the available geological and geophysical data, we can suppose that in regions near stations CHM, KBK, and PDG, the vertical wave guide has smaller velocity contrast than in the Zaili fault region. In this case, *S* waves can approach on the surface almost vertically. Besides that, the topographic contrast and sedimentary layer thickness in these cases (especially for stations CHM and PDG) are much lower than in the Zaili fault region. For these reasons, *S* waves are not

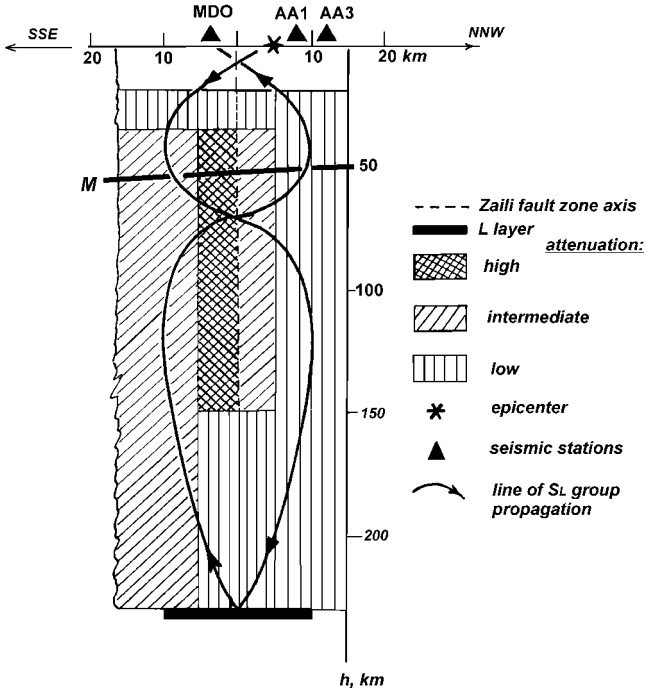

Figure 17. Possible S_L group propagation scheme in the Zaili fault region. The attenuation field structure is from Kopnichev (2000). We suppose that higher attenuation corresponds to lower velocities and vice versa. Note different scales at horizontal and vertical axes.

scattered at the surface, and the S_L group should be horizontally polarized.

Smaller t_m times and T_m periods to the west of 76° E are most likely connected with larger velocities of *S* waves in the upper mantle of this region, compared with those in the Zaili fault region. At the same time, certainly, other possible explanations exist, for example, a decrease in the depth of the *L* layer and its thickness near the Chu depression.

The suggested hypothesis can be checked using two indirect methods. The first method is connected with the usual *S*-coda decay rate in the presence of the vertical wave guide. It is evident that in this case the geometric divergence of the coda amplitudes should be proportional to $t^{-1/2}$, similar to the formation of coda by surface waves (Aki, 1969):

$$A_c \sim \exp(-\pi t/Q_s T)/t^{1/2}. \quad (1)$$

Figure 18 shows general coda envelopes, obtained using recordings from three stations, where the S_L group stands out clearly. The recordings of Aglatas quarry explosions were used for CHM, Kotur–Bulak quarry explosions were used for MDO, and the recordings of two local earthquakes were used for PDG (Table 2). One can see that even taking attenuation into account, the coda decays more slowly than t^{-1}, which corresponds to coda formation by reflections with no wave guide (Kopnichev, 1985), in the first case for $t > 16$ sec, in the second for $t > 30$ sec, and in the third for $t > 25$ sec

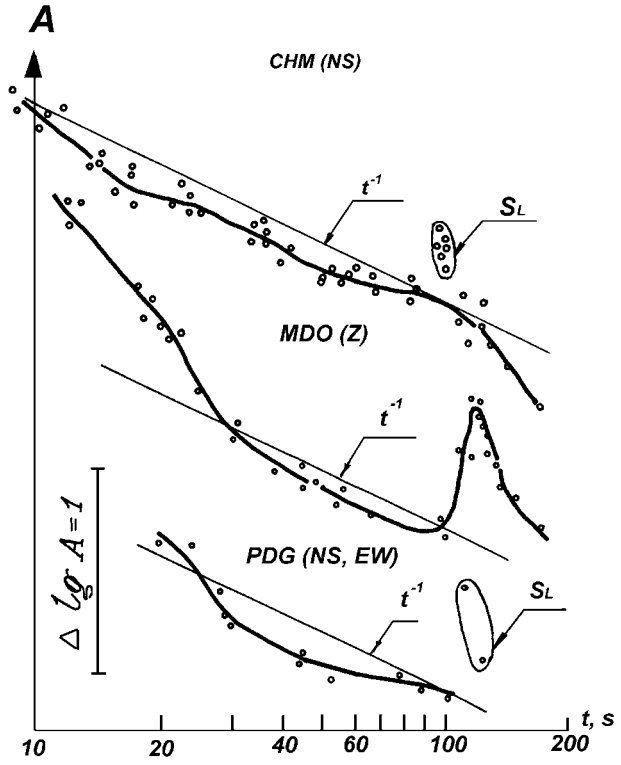

Figure 18. General coda envelopes for different stations; 0.6-Hz filter.

up to $t \sim 100$ sec. Note the much higher coda decay rate for MDO station recordings (in the Zaili fault zone) than for the other stations. Thus, the S coda in these cases attenuates relatively slowly. This does not contradict our hypothesis on the S_L group nature.

The second method is connected with an estimation of the S_L group level relative to S coda at higher frequencies. It is well known that the maximum reflection index for a thin layer can be observed at

$$h_L = \lambda/4, \tag{2}$$

where in our case $\lambda = c_s T_m$ is the prevailing wavelength (at almost vertical incidence) and c_s is the velocity of S waves in the L layer. Simultaneously for the period $T = T_m/2$ in the S coda at the S_L group arrival time we should be able to observe the minimum reflection index. In order to check this conclusion, we determined the maximum amplitudes within the interval of $[t_m - 2$ sec, $t_m + 2$ sec] [let us denote it $A_{SL}(T_m/2)$] with respect to the coda envelopes. The envelopes were constructed using local extrema for the CHISS channel with the central frequency at 1.25 Hz (for the same component, where the maximum amplitude of the S_L group on the 0.6-Hz channel is observed). This corresponds to the period $T = T_m/2$. Let us denote $A_{coda}(t_m)$ the amplitude, linearly approximated at $t = t_m$ between the two closest S_L group local coda extrema measured at the times t_1 and t_2 ($t_1 < t_m < t_2$).

We have analyzed recordings of five earthquakes and explosions at stations CHM, KBK, and PDG, where no dispersion of the S_L group is observed (Fig. 14). In this case the mean value of $\log[A_{SL}(T_m/2)/A_{coda}(t_m)]$ equals -0.25 ± 0.09. So, for the coda period $T = T_m/2$ at the S_L group arrival time one can really observe the amplitude gap, which is an additional piece of evidence supporting the suggested hypothesis.

Estimation of L Layer Parameters

It is rather difficult to estimate the depth of the L layer for the Zaili fault region using t_m values because the velocity contrast in the upper mantle is relatively large and S ray paths in a wave guide are not well known. Therefore, we will conduct the following estimation for the region near CHM, where we can reliably estimate t_m values using recordings of Aglatas quarry explosions (Table 1). Let us assume that the average S-wave velocity in the Earth's crust equals 3.5 km/sec and the thickness of the crust is 45 km. The average velocity of S waves in the Northern Tien Shan upper mantle at depths down to 300 km is about 4.6 km/sec (Roecker *et al.*, 1993). For the Kendyktas range, the c_s value is higher by about 4%, that is, 4.8 km/sec. From these data, we find that the depth of the L layer $H_L \sim 230$ km. If we assume that the uncertainty of velocity estimation is about 0.1 km/sec, then the uncertainty in H_L equals 5 km.

We can estimate the thickness of the L layer using equation (2). Assuming $c_s = 4.8$ km/sec for $T = 1.5$ sec, we find $h_L \sim 1.8$ km.

We can obtain a rough estimate of the index of reflection of S waves from the L layer using the following method. The ratio of S_L amplitude to direct S wave amplitude at the reference distance $r_0 = 10$ km can be simply expressed by

$$A_{SL}/A_S = (r_0/r)^{1/2} \exp(-\alpha_c(r - r_0))N_f V_L, \ \alpha_c = \pi/Q_s c_s T, \tag{3}$$

where r is the path length traveled by the S_L group, α_c is an amplitude attenuation coefficient, which is a sum of a real attenuation and scattering coefficients (Kopnichev, 1985), N_f is a focusing factor, which describes the amplitude increase in the convergence zone, and V_L is the index of reflection from the L layer. Here we do not take into consideration variations of the S-wave radiation pattern because of the averaging of data from different explosions.

From equation (3), we see that there are important factors that can lead to an increase in the amplitude ratio of S_L to S: weak geometric spreading in a wave guide, focusing, and index of reflection V_L, which almost doubles in the case of reflection from a $\lambda/4$ thick layer.

For the double path of S waves to L layer and back, we have $r \sim 460$ km. Using the coda envelopes decay and formula (1), we can estimate α_c. From the plot shown in Figure 18, we obtain $\alpha_c \sim 2{,}1 \times 10^{-3}$ km^{-1}.

Using the recordings of eight explosions at the Aglatas

quarry, we found that the ratio A_{SL}/A_S at the frequency of 0.6 Hz (north–south channel) on average equals $(7 \pm 5.5) \times 10^{-2}$. We should note a large dispersion of this parameter's values, which is mainly connected with *S*-wave radiation pattern variations.

The value of N_f can be estimated from the A_{SL}/A_S ratio. For the Aglatas–CHM path, this value exceeds the minimum by 5 times (Fig. 7). In the first approximation, we can assume that this number 5 corresponds to N_f (actually, using such an approximation, we will most likely underestimate N_f).

Substituting the obtained value into formula (3), we find that V_L for the given path equals 0.24. Taking into consideration an almost doubling of amplitudes at the reflection from the *L* layer, we see that the index of reflection from the top of the layer $\chi_L \sim 0.12$. Taking into consideration what we assumed in order to obtain this value, we should consider this estimate to be only tentative.

We should note that the obtained value of the reflection index is several times smaller than the corresponding estimate for the upper boundary of the sinking lithosphere plate in central Japan, which is a source of fluids and melts rising into the Earth's crust (Obara and Sato, 1988).

On the Nature of the *L* Layer

From the data given by McCamy *et al.* (1962), we find that for our estimate of the reflection index for the vertically incident *S* waves on the *L* layer boundary (for one-phase medium boundaries), the velocity change can be up to 16%–17% and the density change can be up to 11%.

In order to find out the nature of the *L* layer, we should take into consideration the data on the time variations of shear-wave attenuation field structure. As was said before, in the Northern Tien Shan region, such variations can be found in coda at times $t < 135$ sec, which approximately corresponds to the maximum arrival time of the S_L group (Kopnichev, 1998). Based on this, an important conclusion can be made: the lower boundary of the upper mantle, where temporal variations of the attenuation field structure are observed, almost coincides with the *L* layer.

The sufficiently large index of reflection of *S* waves impinging on the *L* layer boundary and the lack of a similar group of reflected longitudinal waves lead to the unambiguous conclusion that the layer is saturated with a liquid phase. The small thickness of the layer and its being joined to the lower boundary of the upper mantle, where rapid time variations of shear-wave attenuation field structure can be observed, allow us to suggest that the liquid phase is not a melt, but some mobile fluid.

The data obtained in this study do not allow us to draw an unambiguous conclusion that the *L* layer underlies only a narrow band along the border between mountains and depressions. Perhaps it covers a much bigger area, but, as we showed earlier, in order to discriminate the S_L group, one needs an existing, markedly subvertical wave guide.

One possible origin of the *L* layer is connected with processes of dehydratation of very dense hydrosilicates in the upper mantle. Liu (1989) introduced the notion of the water line, which is determined by forsterite + enstatite + $H_2O \leftrightarrow$ forsterite + enstatite + A phase reaction, which, in his opinion, should exist under the continents at the depth of about 250 km. Above that line, free water fluids should exist, although in small quantities.

Note that the depth of the *L* layer is close to the Lehmann boundary, which in different regions is situated at depths of 200–250 km (Anderson, 1979).

The data given earlier suggest that the S_L group stands out most clearly in the Zaili fault region. Note that many geological and geophysical parameters suggest that this fault zone is abnormal: it is characterized by a maximum contrast of tectonic movements (Krestnikov *et al.*, 1979), very high heat flow (Vilyaev, 1994), the presence of mantle-derived helium (Polyak *et al.*, 1990), and considerable temporal variations of attenuation field structure (Kopnichev, 1998). All this indicates the presence of a considerable portion of free fluids in this zone. The new data allow us to assume that, at least in the Zaili fault region, the *L* layer is a main source of fluids that rise into the upper mantle and Earth's crust. Let us note that the rise of fluids occurs not everywhere, but mainly where large fault zones intersect and where the maximum time variations of the *S*-wave attenuation field structure are observed (Kopnichev and Sokolova, 1997; Kopnichev, 1998).

Conclusions

1. An abnormal wave group (S_L) stands out clearly against the background of the short-period *S* coda in the Northern Tien Shan region on the recordings of local earthquakes and quarry explosions. This wave group, however, was found only on the recordings of stations installed on the borders between mountain structures and depressions to the north (Chu and Ili).
2. A comprehensive study of velocity and amplitude characteristics of the S_L group shows that its main peculiarities are a very narrow oscillation spectrum (at distances up to 30 km, the periods are 1.5–1.8 sec), variability of velocity and polarization characteristics, and a considerable difference in these parameters for the Zaili fault zone and regions to the west of 76° E and to the east of 79° E.
3. Based on the analysis of experimental characteristics, a hypothesis was brought that the S_L group is formed by shear waves, propagating in a subvertical wave guide and reflected from a thin layer in the upper mantle. It is shown that available data do not contradict this hypothesis.

Acknowledgments

We are grateful to R. T. Beisenbaev and G. G. Schelochkov for providing digital and analog seismic data. We also thank Peter Molnar for valuable comments and correction of the English translation. Helpful comments from Michael Fehler and two anonymous reviewers also greatly improved the manuscript.

References

Aki, K. (1969). Analysis of the seismic coda of local earthquakes as scattered waves, *J. Geophys. Res.* **74,** 615–631.

Anderson, D. (1979). The deep structure of continents, *J. Geophys. Res.* **84,** 7555–7560.

Aptikaeva, O. I., and Yu. F. Kopnichev (1993). Space-time variations of the coda-wave envelopes of local earthquakes in the region of Central Asia, *J. Earthquake Predict. Res.* **2,** 497–514.

Brekhovskih, L. M. (Editor) (1974). *Acoustics of the Ocean*, Nauka, Moscow (in Russian).

Gal'perina, R. M., I. L. Nersesov, and E. I. Gal'perin (1985). Seismic Regime of Alma-Ata City for 1972–1982, IPE, Moscow (in Russian).

Herquel, G., P. Tapponnier, G. Wittlinger, J. Mei, and S. Danian (1999). Teleseismic shear wave splitting and lithospheric anisotropy beneath and across the Altyn Tagh fault, *Geophys. Res. Lett.* **26,** 3225–3228.

Hill, R. N., and A. R. Levander (1984). Resonances of low-velocity layers with lateral variations, *Bull. Seism. Soc. Am.* **74,** 521–537.

Kopnichev, Yu. F. (1985). *Short-Period Seismic Wave Fields*, Nauka, Moscow (in Russian).

Kopnichev, Yu. F. (1998). Variations in the structure of the field of attenuation of shear waves related to pairs of strong earthquakes in Central Asia, *J. Earthquake Predict. Res.* **7,** 139–157.

Kopnichev, Yu. F. (2000). On a fine structure of the Earth's crust and upper mantle at the border of the North Tien Shan, *Doklady AN* **375,** 93–97 (in Russian).

Kopnichev, Yu. F., and I. N. Sokolova (1997). Variations of the Earth rotation speed and geodynamic processes in Central Asia, *Doklady AN* **353,** 386–389 (in Russian).

Krestnikov, V. N., T. P. Beloussov, V. I. Yermilin, N. V. Chigarev, and D. V. Shtange (1979). *Quaternary Tectonics of Pamir and Tien-Shan*, Nauka, Moscow (in Russian).

Levander, A. R., and R. N. Hill (1987). *P-SV* resonances in irregular low-velocity surface layers, *Bull. Seism. Soc. Am.* **75,** 847–864.

Liu, L. (1989). Water, low-velocity zone, and the descending lithosphere, *Tectonophysics* **164,** 41–48.

McCamy, K., R. Meyer, and T. Smith (1962). Generally applicable solutions of Zoeppritz' amplitude equations, *Bull. Seism. Soc. Am.* **52,** 923–955.

Obara, K., and H. Sato (1988). Existence of an *S* wave reflector near the upper mantle of the double seismic zone beneath the southern Kanto district, Japan, *J. Geophys. Res.* **93,** 15,037–15,045.

Polyak, B. G., I. L. Kamensky, A. A. Sultankhodzhaev, I. G. Chernov, L. N. Barabanov, A. K. Lisitsyn, and M. V. Khabarovskaya (1990). Submantle helium in fluids of Southeastern Tien-Shan, *Doklady AN* **312,** 721–725 (in Russian).

Rautian, T. G., and V. I. Khalturin (1978). The use of the coda for determination of the earthquake source spectrum, *Bull. Seism. Soc. Am.* **68,** 923–948.

Roecker, S. W., T. M. Sabitova, L. P. Vinnik, Y. A. Burmakov, M. I. Golvanov, R. Mamatkanova, and. L. Munirova (1993). Three-dimensional elastic wave velocity structure of the western and central Tien Shan, *J. Geophys. Res.* **98,** 15,779–15,795.

Vilyaev, A. V. (1994). Heat flow of seismically active regions in the southeastern Kazakhstan, in *Problems of Earthquake and Seismic Hazard Forecast*, First Edition, Institute of Seismology, Alma-Ata, Kazakhstan, 92–98 (in Russian).

Joint Institute of Physics of the Earth
Russian Academy of Sciences
Kamo Str. 8a
Talgar, Almaty Region
Kazakhstan, 483310
cse@mail.kz
(Y.F.K.)

Manuscript received 2 July 2001.